



Research on Degradation of Dye Acid Red B by $\text{Sr}_2\text{FeMoO}_6$ Synthesized by Microwave Sintering Method

YONG-QING ZHAI*, JING QIAO and MAN-DE QIU

College of Chemistry and Environmental Science
Hebei University, Baoding, 071002, People's Republic of China
zhaiyongqinghbu@163.com

Received 28 July 2011; Accepted 4 October 2011

Abstract: Double perovskite $\text{Sr}_2\text{FeMoO}_6$ was synthesized rapidly by microwave sintering method. The crystal structure of the sample was investigated by XRD. It shows that the as-synthesized sample is $\text{Sr}_2\text{FeMoO}_6$ with tetragonal crystal structure and $I4/mmm$ space group. The test of electrical transport properties shows that the sample exhibits typical semiconductor behavior in the temperature range of 80~300 K. The influence of the dosage of the sample, light irradiation sources, and time on the efficiency of degradation have been studied. The results show $\text{Sr}_2\text{FeMoO}_6$ exhibits excellent degradation activity for dye Acid Red B, the decolorization rate is close to 100% under proper conditions. Meanwhile, a mechanism related to the process of degradation is proposed.

Keywords: Microwave sintering method, $\text{Sr}_2\text{FeMoO}_6$, Degradation, Acid Red B.

Introduction

As is well known, TiO_2 is a stable photocatalyst which can be applied to degrade the wastewater¹. But the band gap of TiO_2 is 3.2 eV, so TiO_2 can only absorb ultraviolet light (UV), which accounts for merely 3% of the entire solar energy. As a result, the degradation reaction is inefficient and the scope of application is limited.

Recently, people pay attention to perovskite-type oxides ABO_3 which shows good catalytic activity *etc.* In perovskite-type oxides ABO_3 , the corner-shared octahedron BO_6 can facilitate the electron transfer and the oxygen transfer, which leads to the oxygen vacancies², and makes ABO_3 an excellent catalyst for the degradation of pollutant. For example, Sun Mengmeng *et al.*³ has found that perovskite-type oxide BaFeO_{3-x} can degrade methyl orange in the dark, and degradation rate can be improved under visible light; Ding Jianjun *et al.*⁴ studied the photocatalytic activities of different kinds of ABO_3 -type oxides ($A=Y, \text{La}, \text{Nd}, \text{Sm}, \text{Eu}, \text{Gd}, \text{Dy}, \text{Yb}$, $B=\text{Al}$, and In) and found YInO_3 and YAlO_3 showed high activities for toluene oxidation. Ding Jianlin *et al.*⁵ synthesized perovskite ReFeO_3 ($\text{Re}: \text{La}, \text{Sm}, \text{Eu}, \text{Gd}$)

and found all these samples exhibited good photocatalytic activity for the degradation of Rhodamine B aqueous solution under visible light irradiation.

At present, double perovskite-type oxides $A_2B'B''O_6$ have attracted great interests because A, B', and B'' atoms can be adjusted within a large range, which makes $A_2B'B''O_6$ show various special performances^{6,7}. Some double perovskite-type oxides exhibits semiconductor behavior, so this type of materials, as a candidate for photocatalysts in degrading the wastewater, should have good potential⁸.

Sr_2FeMoO_6 as a kind of double perovskite-type oxides has attracted considerably scientific and technological interest in recent years owing to its giant magnetoresistance under low field at the room-temperature⁹. But Sr_2FeMoO_6 used for the degradation of organic dyes has not been reported. In this paper, we succeeded in synthesizing Sr_2FeMoO_6 by microwave sintering method, which is an efficient and energy saving technique, and investigated its degradation activity for dye Acid Red B solution.

Experimental

Polycrystalline Sr_2FeMoO_6 was prepared by microwave sintering method. Stoichiometric powders of $SrCO_3$ (A.R.), Fe_2O_3 (A.R.) and MoO_3 (A.R.) were mixed, then ground to ensure homogeneity. Microwave sintering process was divided into two stages. First stage was pre-sintering. The mixture was pressed into tablets at 10 MPa and then placed into a corundum crucible inside a large covered ceramic crucible. The space between the corundum and the ceramic crucible was filled with MnO_2 as a heating medium. The crucibles were placed into a Galanz WD700 (L23) microwave oven, and sintered for 30 min under the power of middle-high fire. After natural cooling, the precursor was obtained. Second stage was reduction. The precursor was finely ground, then pressed into tablets again. The tablets were placed into corundum crucible and buried in the granular activated carbon as reductant. The crucible was covered and put into a big ceramic crucible with MnO_2 , then placed into the same microwave oven and sintered for 30 min under the power of middle-high fire. After natural cooling, the final product was gained.

Degradation Reaction

The degradation reaction was carried out in 250 mL beaker containing 50 mL dye Acid Red B solution (its concentration was 20 mg/L) and some amount of Sr_2FeMoO_6 . The suspension was stirred for some time and then filtered. With distilled water as reference solution, the absorbance of the filtrate was measured at the maximum absorption ($\lambda_{max}=515$ nm) of the dye to calculate the decolorization rate (*De*) of dye Acid Red B. $De=(1-A/A_0)\times 100\%$, where *A* shows final absorbance and A_0 shows initial absorbance of dye solution. The decolorization rate of dye was used to characterize the degradation activity of Sr_2FeMoO_6 .

Characterization

The crystal structure of the sample was examined by X-ray powder diffraction (XRD) using a D8 Advance diffractometer with Cu $K\alpha$ radiation (40 kV \times 40 mA), $\lambda = 0.154\ 060$ nm at room temperature, that was made by the company of Bruker in Germany. Electrical transport properties (ρ -T) were determined by a standard four-probe DC method. The IR spectra were recorded on a Nicolet 380 Fourier transform infrared spectroscopy (FT-IR) in order to make sure whether the dye is absorbed on the surface of the sample or degraded completely. Absorption curve and absorbance of dye solution were measured by a TU-1810 UV-Vis Spectrophotometer (UV-Vis).

Results and Discussion

Analysis of Phase Structure

Figure 1 shows the XRD pattern of as-synthesized sample. The diffraction peaks can be indexed to $\text{Sr}_2\text{FeMoO}_6$ in a tetragonal system with space group $I4/mmm$ by the Jade5 program, and unit cell parameter is $a=0.5587\text{ nm}$, $c=0.7894\text{ nm}$. The appearance of the superstructure reflection (101) around 19.4° indicates the order degree of the Fe and Mo cations in a certain extent which occupy the B' and B'' site, respectively, in $A_2B'B''O_6$ with the alternating arrangement of FeO_6 and MoO_6 octahedra, and form Fe-O-Mo bond. Moreover, an extremely weak diffraction peak appears around 44.6° , which is indexed to Fe. This indicates trace Fe exists in the sample. The reason is that the precursor directly contacted with activated carbon in the second stage, reducing agent was excessive and reducing atmosphere was abundant, so a little amount of Fe^{3+} was reduced to simple substance Fe.

In our experiment, the double perovskite-type oxide $\text{Sr}_2\text{FeMoO}_6$ was synthesized successfully by microwave sintering method within only 1 h. Compared to traditional high temperature solid state sintering method (calcination temperature is generally about 1200°C and calcination time is $12 \sim 24\text{ h}$)¹⁰, this method has the following advantages, energy saving, high efficiency, easy operation, and so on.

Analysis of Electrical Transport Behavior

Double perovskite $\text{Sr}_2\text{FeMoO}_6$ can exhibit insulating, semi-conducting, or metallic behavior, depending on synthesis conditions¹¹. In our present work, the variations in resistivity of $\text{Sr}_2\text{FeMoO}_6$ as a function of temperature under zero magnetic field are given in Figure 2. It can be seen that the sample exhibits typical semiconducting behavior ($d\rho/dT < 0$) in the temperature range of $80 \sim 300\text{ K}$. Below 150 K , resistivity ρ reduces significantly with the increase of temperature; above 150 K , reduces slowly.

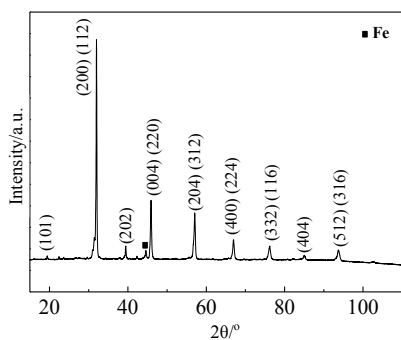


Figure 1. XRD pattern of $\text{Sr}_2\text{FeMoO}_6$.

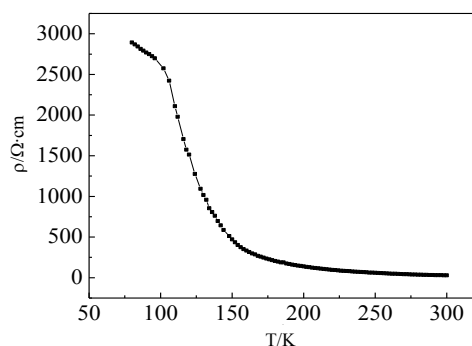


Figure 2. Temperature dependence (T) of resistivity (ρ).

Degradation activity of $\text{Sr}_2\text{FeMoO}_6$ for dye Acid Red B solution

Effect of Dosage on Decolorization Rate

Under the same conditions (60 min under ultraviolet irradiation), the effect of dosage of $\text{Sr}_2\text{FeMoO}_6$ on decolorization rate is shown in Figure 3. It can be seen that the dosage of $\text{Sr}_2\text{FeMoO}_6$ affects the decolorization rate remarkably. The decolorization rate increases with the dosage of $\text{Sr}_2\text{FeMoO}_6$, and the decolorization rate is about 97% when the dosage is

100 mg/50 mL. After that, the decolorization rate is essentially the same. Therefore, the optimum dosage of $\text{Sr}_2\text{FeMoO}_6$ is 100 mg/50 mL.

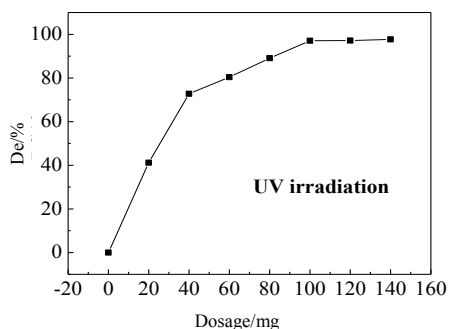


Figure 3. Relationship between dosage of $\text{Sr}_2\text{FeMoO}_6$ and decolorization rate.

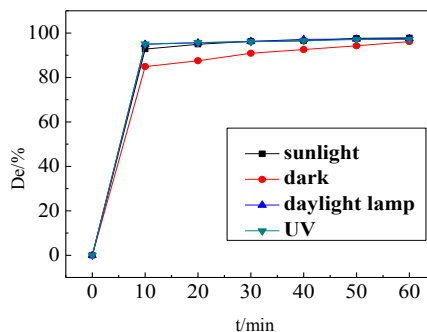


Figure 4. Relationship between irradiation time and decolorization rate.

Effect of Light Sources and Reaction Time on Decolorization Rate

With the same dosage 100 mg of $\text{Sr}_2\text{FeMoO}_6$, the effect of reaction time under different light sources (ultraviolet lamp, daylight lamp, sunlight, and dark condition) on the decolorization rate is shown in Figure 4. It can be seen that the changing trend of decolorization rate is basically consistent under different light sources. The decolorization rate can reach about 95%, 95%, 93%, respectively, under ultraviolet lamp, daylight lamp, sunlight only within 10 min irradiation, after that decolorization rate increases slowly. When reaction time is 30 min, the decolorization rate is close to 100%. In dark condition, the reaction rate is relatively slow, the decolorization rate is about 85% within 10 min and after that decolorization rate increases slowly, but the decolorization rate is also close to 100% when reaction time is 60 min. Thus, $\text{Sr}_2\text{FeMoO}_6$ whether in light or dark all exhibits good degradation activity for dye Acid Red B and the light irradiation can accelerate the decolorization reaction rate.

Decoloring Mechanism

UV-Vis spectra of the filtrate after degrading reaction was measured and contrasted with that of initial Acid Red B (constitutional formula is shown in Figure 5) solution. From Figure 6, it can be seen that the absorption curve (a) of initial solution has two obvious absorption peaks. Based on spectrum theory, the strong absorption peak at 515 nm in visible region is caused by of the conjugated system of azo bond; the absorption peak at 322 nm in ultraviolet region is due to naphthalene connected with the azo bond. It can be seen from curve (b) that characteristic absorption peak at 515 nm of the dye solution has disappeared completely after the degrading reaction, and the intensity of absorption peak at 322nm also decreases significantly.

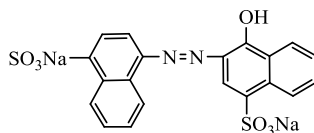


Figure 5. Constitutional formula of Acid Red B.

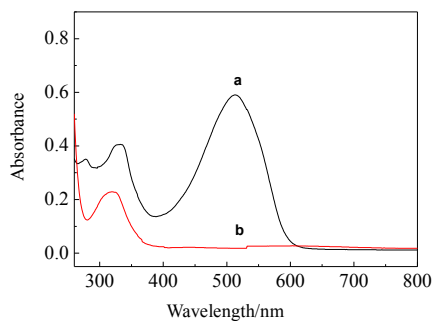


Figure 6. UV-Vis spectra of the initial Acid Red B solution(a) and the filtrate after degrading reaction (b).

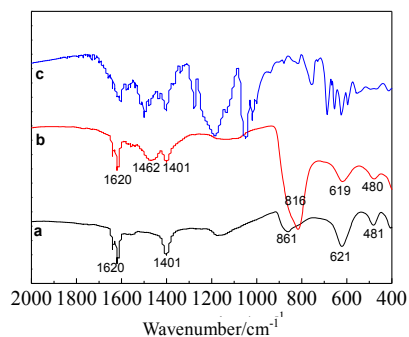


Figure 7. IR spectra of $\text{Sr}_2\text{FeMoO}_6$ (a), the solid sample after degrading reaction (b) and Acid Red B(c).

In order to explain the reason for the decolorization of dye, IR spectra of $\text{Sr}_2\text{FeMoO}_6$, the solid sample after degradation reaction and the dye Acid Red B were measured and contrasted. From Figure 7, it can be seen that there are not characteristic peaks of dye Acid Red B in IR spectrum of the solid sample after degrading reaction. It indicates that the dye molecules weren't adsorbed by the solid sample. It is proved that the decolorization of dye Acid Red B is caused by the degradation of dye under the existence of $\text{Sr}_2\text{FeMoO}_6$, not by adsorption. In IR spectra of the solid samples before and after degrading reaction (curves a and b), the absorption bands around 1400 and 1620 cm^{-1} are due to H-O-H vibration of H_2O molecules. The reason is that surface of the sample absorbed H_2O molecules in the air. In IR spectrum of $\text{Sr}_2\text{FeMoO}_6$ (curve a), there are a strong absorption band between 600 and 700 cm^{-1} and two relatively weak bands at about 861 and 481 cm^{-1} . The strong absorption band centered at about 621 cm^{-1} is assigned to Mo-O anti-symmetric stretching mode of MoO_6 -octahedra¹² and the relatively weak absorption band at about 861 cm^{-1} is ascribed to Mo-O symmetric stretching mode. In $\text{A}_2\text{B}'\text{B}''\text{O}_6$ double perovskite, the highly charge B-cation octahedra, the MoO_6 , act as independent groups, the vibration spectrum, therefore, arises from such MoO_6 octahedra. Mo-O symmetric stretching mode of MoO_6 -octahedra at about 861 cm^{-1} is usually an infrared inactive vibration, but in double perovskite, both B' and B'' ions exist in B sites, it becomes partially allowed due to lowering site symmetry¹². The absorption band at 481 cm^{-1} is ascribed to Fe-O vibration absorption of FeO_6 octahedra. In IR spectrum of the solid sample after degrading reaction (curve b), the vibration absorption band of Mo-O is moved to about 816 cm^{-1} and the intensity is enhanced. This indicates that the valence of Mo has changed and risen to +6¹³. The absorption band around 619 cm^{-1} can still be assigned to the anti-symmetric stretching mode of MoO_6 octahedra, but the intensity is weakened which indicates the content of $\text{Sr}_2\text{FeMoO}_6$ decreases. The absorption band around 480 cm^{-1} can still be ascribed to Fe-O vibration absorption. And there is a new absorption band around 1462 cm^{-1} , which arises from CO_3^{2-} vibration¹⁴. It indicates that the solid sample has been changed after decoloring reaction.

In addition, it is found that the color of solid sample changed from black into khaki after $\text{Sr}_2\text{FeMoO}_6$ was added into the dye solution. In order to understand this phenomenon, the phase structure of the solid sample after reaction was analyzed and shown in Figure 8. From Figure 8, it can be seen that the phase structure of solid sample has been changed indeed. Most of $\text{Sr}_2\text{FeMoO}_6$ has been changed into SrMoO_4 (JCPDS No. 08-0482), SrCO_3 (JCPDS No. 05-0418) and Fe_2O_3 (JCPDS No. 33-0664). This may be due to the hydrolysis reaction of

$\text{Sr}_2\text{FeMoO}_6$ after it was added into the dye solution. According to the results of XRD analysis, the hydrolysis reaction process was presumed as follows:



The generated $\text{Sr}(\text{OH})_2$ contacted with CO_2 in air and reacted, coming into being SrCO_3 , while FeO was oxidized to Fe_2O_3 . After decoloring experiment, the trace Fe still exists in the solid sample.

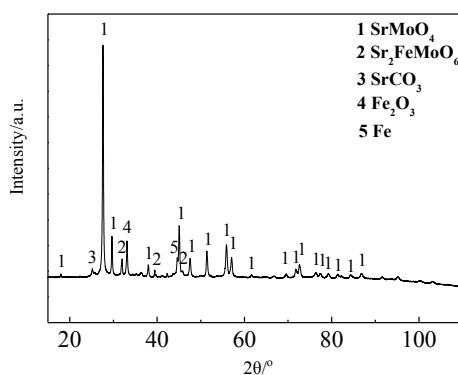
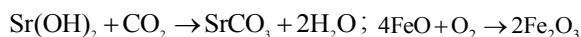


Figure 8. XRD pattern of the solid sample after degrading reaction.

In experiment, it was observed that the color of dye and solid sample could be changed immediately after $\text{Sr}_2\text{FeMoO}_6$ was put into the solution. This shows that the hydrolysis and degradation reactions occurred almost simultaneously, and the process was complex. Based on the experimental phenomenon, we speculate that the decolorizing mechanism is as follows: double perovskite $\text{Sr}_2\text{FeMoO}_{6-\delta}$ was prepared in reducing atmosphere, so there are some oxygen vacancies. Due to the positive electrical property of oxygen vacancies, the OH^- and H_2O adsorbed on the surface of $\text{Sr}_2\text{FeMoO}_{6-\delta}$ particles are easy to be oxidized to highly active hydroxyl radicals ($\cdot\text{OH}$). $\cdot\text{OH}$ is a kind of strong oxidants, it can oxidize the adjacent dye molecules and the $\cdot\text{OH}$ can also spread to the solution and oxidize other dye molecules, making them degrade into inorganic small molecule, so as to achieve the purpose of decolorization. In addition, the double perovskite $\text{Sr}_2\text{FeMoO}_{6-\delta}$ exhibits semiconducting behavior (shown in Figure 2), so the electrons in the valence band can be excited and hopped to the conduction band under the external light irradiation, generating photoinduced electrons in the conduction band and photoinduced holes (h^+) in the valence band, i.e., forming the electron-hole pairs. The oxygen vacancies of $\text{Sr}_2\text{FeMoO}_{6-\delta}$ can also play a role of the trap to capture the photoinduced electrons¹⁵, thus can inhibit the recombination of photoinduced electrons and holes effectively. Therefore, light irradiation is conducive to the formation of positive electrical holes and can accelerate the generation of $\cdot\text{OH}$ from OH^- and H_2O , relevant reactions are as follows: $\text{h}^+ + \text{OH}^- \rightarrow \cdot\text{OH}$, $\text{h}^+ + \text{H}_2\text{O} \rightarrow \cdot\text{OH} + \text{H}^+$. This results in the further increase of the decolorization reaction rate.

Conclusion

The double perovskite $\text{Sr}_2\text{FeMoO}_6$ was synthesized by microwave sintering method. Compared to traditional high temperature solid state sintering method, the reaction time is shortened greatly and energy consumption is reduced effectively. $\text{Sr}_2\text{FeMoO}_6$ exhibits high degradation activity for dye Acid Red B. When the initial concentration of the dye is 20 mg/L, the optimum dosage is 100 mg/50 mL, the decolorization rate is close to 100% in 30 min under light irradiation or 60 min with no light. The decoloring mechanism is presumed as follows: the positive electrical oxygen vacancies in $\text{Sr}_2\text{FeMoO}_6$ can oxidize H_2O and OH^- absorbed on the surface of $\text{Sr}_2\text{FeMoO}_6$ particle into high activity hydroxyl radicals $\cdot\text{OH}$. Then $\cdot\text{OH}$ oxidizes the dye molecules to achieve the purpose of decolorization. Photoholes can be generated under light irradiation, accelerating the formation of $\cdot\text{OH}$. So the degradation reaction rate can be improved by light irradiation. Moreover, a new phenomenon, hydrolysis reaction of $\text{Sr}_2\text{FeMoO}_6$, is found. The final products are SrMoO_4 , SrCO_3 and Fe_2O_3 .

Acknowledgment

This study was supported by National Natural Science Foundation of China (No. 50672020) and Technology Plan Project of Science and Technology Department of Hebei Province (China, No. 10276732). We gratefully acknowledge their supports during the study.

References

1. Fujishima A, Rao T N, and Tryk D A, *J Photochem Photobiol C: Photochem Rev.*, 2000, **1(1)**, 1-21.
2. Kotomin E A, Merkle R, Mastrikov Y A, Kuklja M M, and Maier J, *ECS Trans.*, 2011, **35(1)**, 823-830.
3. Sun M M, Jiang Y S, Li F F, Xia M S, Xue B, and Liu D R, *Mater. Trans., JIM*, 2010, **51(11)**, 1981-1989.
4. Ding J J, Bao J, Sun S, Luo Z L, and Gao C, *J Comb Chem.*, 2009, **11(4)**, 523-526.
5. Ding J L, Lü X M, Shu H M, Xie J M, and Zhang H, *Mater Sci Eng B*, 2010, **171(1~3)**, 31-34.
6. Hu Y C, Ge J J, Ji Q, Jiang Z S, Wu X S, and Cheng G F, *Mater Chem Phys.*, 2010, **124(1)**, 274-280.
7. Park B G, Jeong Y H, Park J H, Song J H, Kim J H, Noh H J, Lin H J, and Chen C T, *Phys Rev B: Condens Matter*, 2009, **79(3)**, 035105 1-8.
8. Hatakeyama T, Takeda S, Ishikawa F, Ohmura A, Nakayama A, Yamada Y, Matsushita A, and Yea J, *J Ceram Soc Jpn.*, 2010, **118(2)**, 91-95.
9. Huang Y H, Yamauchi H, and Karppinen M, *Phys Rev B: Condens Matter*, 2006, **74(17)**, 174418 1-3.
10. Tomioka Y, Okuda T, Okimoto Y, Kumai R, Kobayashi K I, and Tokura Y, *Phys Rev B: Condens Matter*, 2000, **61(1)**, 422-427.
11. Feng X M, Liu G Y, Huang Q Z, and Rao G H, *Trans Nonferrous Met Soc China*, 2006, **16(1)**, 122-126.
12. Lavat A E and Baran E J, *Vib Spectrosc*, 2003, **32(2)**, 167-174.
13. Thongtem T, Phuruangrat A, and Thongtem S, *Mater Lett.*, 2008, **62(3)**, 454-457.
14. Chen Y H, Tong Y, Wei Y J, Liu X Q, and Meng G Y, *Chin J Rare Metal*, 2007, **31(1)**, 57-62.
15. Jing L Q, Yuan F L, Hou H G, Xin B F, Cai W M, and Fu H G, *Sci China Ser B*, 2005, **48(1)**, 25-30.

